

# Physical mechanism for in-plane molecular orientation in polymer-dispersed ferroelectric liquid crystals

Min Young Jin,<sup>1</sup> You-Jin Lee,<sup>1</sup> Kyehun Lee,<sup>2</sup> Sin-Doo Lee,<sup>3</sup> and Jae-Hoon Kim<sup>1</sup>

<sup>1</sup>*Department of Electronics and Computer Engineering, Hanyang University, Seoul 133-791, Korea*

<sup>2</sup>*Samsung Electronics Co., Ltd., Giheung, Kyungki 449-712, Korea*

<sup>3</sup>*School of Electrical Engineering, Seoul National University, Seoul 151-742, Korea*

(Received 26 September 2005; published 14 March 2006)

The physical mechanism of liquid crystal (LC) alignment in ferroelectric LC (FLC) droplets dispersed in a photocurable polymer matrix was studied. The orientational ordering of both FLC molecules and the polymer matrix was induced by a rubbed polyimide alignment layer. There existed an optimum FLC droplet size for the production of uniformly oriented molecules and smectic layers for maximum electro-optic modulation. The alignment quality was critically dependent on the droplet size, shape, the helical pitch, and the phase transition sequence of the FLCs. The molecular structure formed inside the FLC droplets resulted from a delicate balance between the elastic energy stored in a restricted geometry and surface interactions at the FLC-polymer interface.

DOI: [10.1103/PhysRevE.73.031703](https://doi.org/10.1103/PhysRevE.73.031703)

PACS number(s): 61.30.-v, 61.41.+e

## I. INTRODUCTION

Inhomogeneous composite materials consisting of liquid crystals and polymers have attracted considerable attention as a means of gaining a basic understanding of the confinement effect and for the development of practical applications in flat panel displays [1–6]. One such composite material is polymer-dispersed liquid crystals (PDLCs) made up of micrometer-sized nematic liquid crystal (NLC) droplets formed in a continuous polymer matrix. The matrix can be switched between an intense scattering state and a transparent state by the application of an external electric field. It has benefits of relatively wide viewing characteristics and high brightness. However, a PDLC exhibits slow response and low contrast, limiting its applications in high-performance displays. In order to overcome these problems, more rapid switching has been achieved in polymer-dispersed ferroelectric liquid crystals (PDFLCs) [7–10].

From the viewpoint of alignment, there is a large difference between a PDLC and a PDFLC. As previously described, PDLC devices use a scattering mode and therefore do not need alignment. However, PDFLC devices are operated by the collective behavior of liquid crystal molecules. That is, they use a birefringence mode, which means that the alignment of the ferroelectric liquid crystal molecules in the droplets is of utmost importance. To date, there are two kinds of alignment methods currently used. One method uses shear stress [7] and the other employs the rubbing of the alignment layer [10]. In the shear alignment method, some problems arise such as droplet asymmetry and lower reproducibility, which is an obstacle in mass production applications. Alternatively, the rubbing method is more suitable to practical applications of mass production due to its droplet symmetry, good reproducibility, and the ease with which droplet size may be controlled. However, in the rubbing method, the mechanism by which the droplets' liquid crystal molecules align in the rubbed layer is still unclear.

The physical properties of the PDLCs are generally affected by a number of parameters such as compatibility be-

tween the polymer matrix and the LC used, the mixing ratio of the two materials, the droplet size and shape, and the resultant dielectric properties. Of particular importance are the anisotropic interfacial interactions of the LC droplets in the restricted geometry polymer matrix, which depend primarily on their chemical and interfacial ordering properties.

Because of the intrinsic molecular chirality and layering in ferroelectric liquid crystals (FLCs), the physical mechanism for the molecular ordering is more complex than that of PDLCs. In addition to polarization reversal, the helix unwinding process and the collective molecular rotation lead to an electro-optic (EO) effect in the PDFLCs. Therefore, it is important to study the PDFLCs under various conditions, to understand the alignment mechanism of the FLC droplets and the relevant surface phenomena at the polymer/LC interface [4]. Moreover, control of the electro-optic response by means of alignment is a subject of interest for many practical applications.

In this paper, we studied the molecular alignment and EO responses of PDFLCs for various droplet sizes. We will describe the alignment mechanism of ferroelectric liquid crystal molecules in the polymer droplets both experimentally and through numerical calculations.

## II. EXPERIMENT

The PDFLCs consisted of FLC droplets dispersed in a polymer matrix. We made FLC droplets in the polymer matrix by the polymerization-induced phase separation (PIPS) method, in which the LCs are homogeneously mixed with prepolymer and a phase separation takes place during the photopolymerization by ultraviolet (uv) illumination [11,12]. The FLC materials used in this study are CS1017 and CS1024 (Chisso Corp.). One of the FLC materials (CS1017) has a tight pitch (1  $\mu\text{m}$ ), and the other (CS1024) has a relatively long helical pitch (20  $\mu\text{m}$ ) in the smectic- $C^*$  ( $\text{Sm } C^+$ ) phase. Both of them have the same phase sequence  $\text{Sm } A\text{-Sm } C^*$ . As will be discussed later, the helical pitch greatly influ-

ences the quality of the alignment as well as the EO responses. The matrix polymer material was NOA 65 (Norland uv-curable optical adhesive 65), a blend of monomers, oligomers, and a photoinitiator. The uv-curable prepolymer and LC were mixed with an 8:1 weight ratio at the isotropic phase temperature (120 °C), and were mixed on a stirplate to ensure uniformity.

The sample cell was made up of conductive indium tin oxide-coated glasses, which were treated with polyimide. The thickness of the polyimide layer was about 300 Å, and both glass surfaces of the cell were unidirectionally rubbed to promote the alignment of the polymer matrix as well as LC droplets. The cell gap was maintained by glass spacers with a thickness of 10 μm. When the cell gap is larger than 10 μm, liquid crystal alignment in the droplet is hardly affected by the surface alignment layer. On the other hand, when the cell gap is smaller than 10 μm, it is hard to control the droplet size. Therefore we fixed the cell gap at 10 μm. The mixing and injection temperatures were held at 120 °C, far above the nematic-isotropic transition temperature of the pure liquid crystal. The samples were kept at 120 °C for 10 min prior to uv irradiation to reduce shear effects. Without this process, the FLCs would align along the direction of shear flow caused by the injection. Moreover, these thermal processes enhanced the spatial uniformity of the PDFLC droplets, compared to samples without the thermal treatment. The optimum conditions, however, were dependent on the material properties of the PDFLCs such as the relative viscosity of the FLC and prepolymer.

Electric contacts were made directly to the internal surfaces of the glasses to apply the external electric field. The sample cells were mounted in a microfurnace for thermal study and the alignment of both the polymer and the LC droplets was determined by an optical polarizing microscope. The EO response of the PDFLCs to an external electric field was measured by monitoring the change in the light intensity transmitted through the sample cell between crossed polarizers. The sample cell was placed such that one of the crossed polarizers was at an angle of 22.5° with respect to the cell's optic axis, to obtain maximum transmission through the cell. The details of the experimental setup have been reported elsewhere [9]. The PDFLCs behaved essentially as uniaxial slabs since biaxiality in our geometry was weak at optical frequencies.

We used a photoelastic modulator (PEM), PEM90 of Hinds Inc., with a fused silica head and a He-Ne laser for optical phase retardation measurements. The PEM was placed between two crossed polarizers with its optical axis at 45° to the direction of polarization. The signal from the photodetector was fed into a lock-in amplifier for ac measurement and a digital multimeter for dc measurement. The lock-in amplifier was tuned to a 50 kHz reference signal from the PEM. The beam was incident along the surface normal, and the signal was measured while rotating the sample with respect to the surface normal. The sensitivity of this method allowed the measurement of phase retardations as small as 0.01°.

The dielectric constant was measured by an impedance analyzer (HP 4192A of Hewlett Packard Co.). The cell was mounted in a Mettler FP90 microfurnace for tempera-

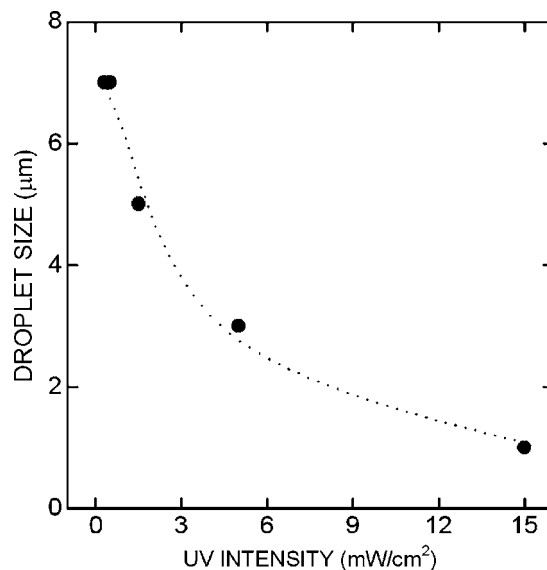


FIG. 1. Control of droplet size by changes in uv irradiation intensity.

ture control, and temperature fluctuations were held to approximately 0.1 °C.

### III. RESULTS AND DISCUSSIONS

To study the size effect of the PDFLCs on their alignment and EO properties, we prepared five different droplet sizes of approximately  $\rho=1, 3, 5,$  and  $7 \mu\text{m}$  in diameter, by changing the uv irradiation intensity from 0.1 to 15 mW/cm<sup>2</sup> using CS1024 compounds. Figure 1 shows the results of controlling droplet size control by varying uv intensity. Droplet size decreased with increasing uv light intensity. Since the polymerization rate of the prepolymer increased with increasing irradiated uv intensity, the high intensity produced small droplets [11,12]. The smectic A-smectic C\* phase transition temperature  $T_{AC^*}$  was shifted 5–10 °C lower than that of the bulk FLC samples due to the confinement effects in a restricted geometry [13,15]. We note that the increased shifts in  $T_{AC^*}$  correlated with decreasing droplet size [14].

The molecular alignment for various droplet sizes through measurements of transmitted intensity was studied with the samples. When the samples were rotated between the crossed polarizers with respect to the surface normal, the transmitted intensity  $T$  varied between  $T_{max}$  and  $T_{min}$  because of the macroscopic birefringence of the sample. The magnitude of this variation in transmittance intensity characterizes the quality of the molecular alignment in the PDFLC droplets. Figure 2 shows the experimental results of  $\Delta T=T_{max}-T_{min}$  as a function of rotating angle ( $\theta$ ) between the front polarizer and the rubbing direction of the sample. In Fig. 2, the open circular, triangular, and filled circular symbols represent  $\rho=1, 3,$  and  $7 \mu\text{m}$ , respectively. For comparison, the results of a well-aligned bulk FLC sample (open squares) and a PDFLC (filled squares) sample using an unrubbed polyimide alignment layer are shown. From these results, it was found that the transmitted intensities of the bulk FLC sample had maximum values near  $\pi/4$  and  $5\pi/4$  and minimum at 0 and  $\pi/2$ .

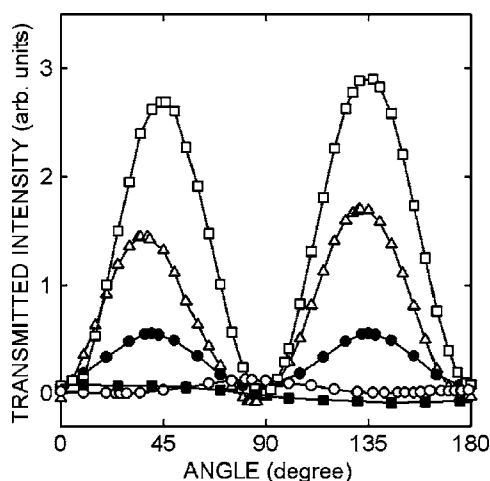


FIG. 2. Transmitted intensities as a function of the rotating angle for several droplet sizes. The open circles, open triangles, and filled circles represent  $\rho=1, 3, \text{ and } 7 \mu\text{m}$ , respectively. Well-aligned bulk FLC samples and unrubbed PDFLC samples are represented by the open squares and filled squares, respectively.

This is a general behavior of homogeneously aligned FLCs between the crossed polarizers. However, no angular dependence was observed in the unrubbed PDFLC sample, which indicates that there was no effective alignment of the FLC molecules or the layers. In contrast, the rubbed PDFLCs showed the same behavior as that of the bulk FLC sample. It was evident that the FLC molecules as well as the smectic layers were aligned in the droplet, which suggested that the rubbing effect was transferred to the droplet through the polymer matrix, as will be discussed later. It is interesting to note that the PDFLC sample of  $3 \mu\text{m}$  droplet size had the maximum transmittance;  $\Delta T$  increased with increasing the droplet size to  $3 \mu\text{m}$ , and then decreased with further increases greater than  $3 \mu\text{m}$ . This indicates that, in the case of our PDFLC samples, an optimum droplet size existed for optimal alignment.

Before studying the optimum droplet size conditions, the alignment mechanism in the droplets was considered. To find the rubbing effect on the alignment, the birefringence of the sample was measured for pure NOA 65 in the rubbed cell. Figure 3 shows the phase retardation as a function of angle rotation for various uv curing times, in which the rotating axis is normal to the glass surface. In Fig. 3, filled circular, triangular, and square symbols represent curing times of 0, 30, and 150 s, respectively. The open circular symbols denote a 500 s curing time. From these results we found that the birefringence of the sample was increasing with increasing curing time. It was also found that the extraordinary optic axis coincided with the rubbing axis. This indicated that the polymer was aligned along the rubbing axis during polymerization. Figure 4 shows the results of the dielectric measurements of pure NOA 65 in rubbed and unrubbed cells. The capacitance of the unrubbed cell gradually increased with increasing uv exposure time, and had a saturated value over 1300 s, which meant that the polymerization process was complete. In the case of the rubbed cell, however, the capacitance rapidly decreased and reached a minimum value after

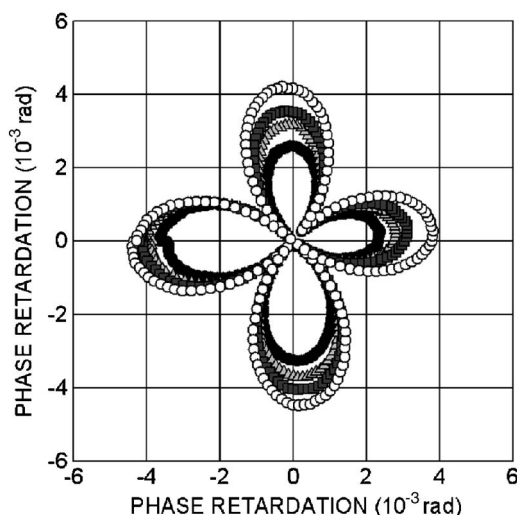


FIG. 3. Phase retardation for pure NOA 65 in a rubbed cell as a function of rotation angle. The filled circular, triangular, and square symbols represent curing times of 0, 30, and 150 s. The open circular symbols denote a 500 s curing time.

approximately 100 s. This sharp decrease was due to the polymer chain alignment by the rubbed polyimide substrate. It was consistent with the birefringence measurements. For longer uv exposures, the capacitance dramatically recovered and saturated within 500 s. This meant that the polymer chain in the bulk was almost the same as that of the unrubbed cell. To explain this phenomenon more clearly, we considered a simple model of polymerization. We assumed there to be two serially connected polymer layers, one ordered by an alignment layer and the other a random polymerized layer. In addition, we also assumed that there is dielectric anisotropy in the cured polymer between the chain alignment direction along the rubbed surface and its normal direction, and that the prepolymers absorb uv light, which

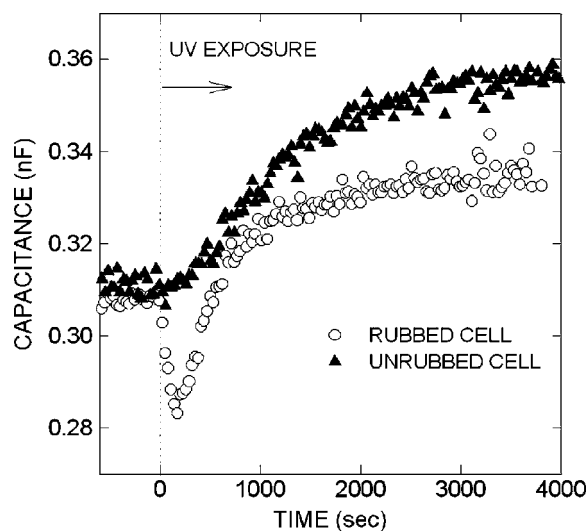


FIG. 4. Capacitance for pure NOA 65 in rubbed and unrubbed cells as a function of uv exposure time. The filled triangles and open circles represent the unrubbed and rubbed cells, respectively. The uv intensity is  $1 \text{ mW/cm}^2$ .

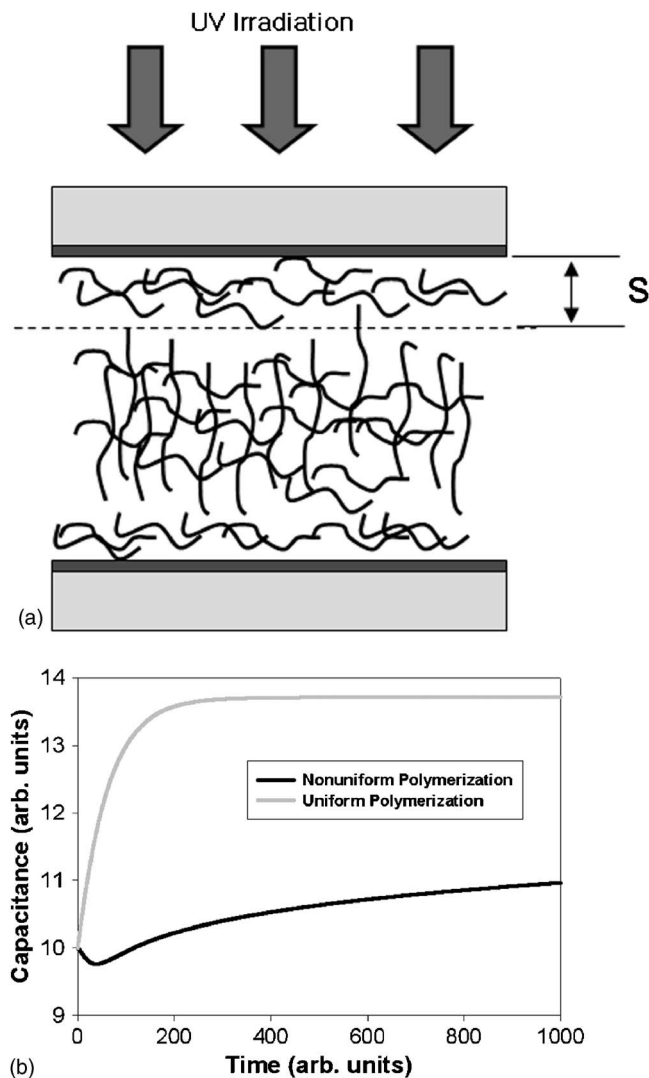


FIG. 5. (a) A schematic diagram of our calculation model of polymerization. (b) Results of numerical calculations for the rubbed and unrubbed alignment layer.

results in an intensity gradient along the substrate normal direction. That is, the polymers on the illuminated side are the first to polymerize. Figure 5(a) shows a schematic diagram of our calculation model. In the figure,  $s$  is the effective surface polymerization region which was affected by the rubbed alignment layer, and isotropic polymerized polymers occupy the other region of  $d-s$ . From the above assumption, we can write the dielectric constant as a function of time:

$$\frac{d}{\epsilon(t)} = \int_0^s \frac{1}{(\epsilon_a - \epsilon_b)\alpha(t)} dz + \int_s^d \frac{1}{(\epsilon_i - \epsilon_b)\alpha(t)} dz + \epsilon_b \quad (1)$$

where  $\epsilon$  is the dielectric constant,  $t$  is the time,  $d$  is the cell gap, and the subscripts  $b, a, i$  correspond to before polymerization, after polymerization with chain alignment, and isotropic polymerization, respectively. The degree of polymerization  $\alpha(t)$  is given by [18]

$$\alpha(t) = 1 - \exp(-kt) \quad (2)$$

which is uniform polymerization, that is, the polymerization rate is the same anywhere. We here introduce the uv intensity gradient  $k$ , which is the polymerization rate, depending on the spatial coordinate  $z$  whose axis is normal to the substrate. The  $k(z)$  function has the following dependence:

$$\frac{\partial I}{\partial z} = -aI, \quad (3)$$

$$k(z) = \beta I(z), \quad (4)$$

where  $I$  is the uv intensity at position  $z$ ,  $a$  is the absorption coefficient of the prepolymer and/or polymer, and  $\beta$  is the rate of polymerization. Figure 5(b) shows the simulation results for the above coupled Eqs. (1)–(4). Several parameters used in this simulation are  $\epsilon_b=10.0$ ,  $\epsilon_a=5.0$ , and  $\epsilon_i=14$ . The negative value of  $\epsilon_a - \epsilon_b$  was crucial in obtaining the same behavior as depicted in Fig. 4. Although we assumed the same dielectric anisotropy and surface region  $s$ , except for nonuniform polymerization, as shown in Fig. 5(b), the dip in dielectric measurement did not appear. It is clear that the existence of the dip in Fig. 4 was due to the early stages of surface polymerization with chain alignment, which could not be obtained from uniform polymerization. From the results, we found that the LC molecules and layers were aligned by the aligned polymer near the surface which was promoted by the rubbed surface. But it is believed that there were some other effects of the FLC molecules and layers in the droplets in their alignment. One of the effects is related to droplet properties such as shape and size. The other comes from the material properties of pure FLCs such as helical pitch, tilt angle, and phase sequences. From a technical point of view, the former effect is very important to achieving uniform alignment because of the droplets reproducibility.

In order to find the droplet shape and distribution in the polymer matrix, the cross-sectional morphology was observed by scanning electron microscopy (SEM) as shown in Fig. 6. Figures 6(a)–6(c) represent the SEM images of 1, 3, and 7  $\mu\text{m}$  samples, respectively. It is interesting that the droplets of 1  $\mu\text{m}$  were distributed uniformly between the two glass plates, though those of 3 and 7  $\mu\text{m}$  were distributed on both glass plates. This indicated that the alignments of the 3 and 7  $\mu\text{m}$  samples were achieved by both the aligned polymer and the rubbed surface. For the 1  $\mu\text{m}$  sample, however, most of the droplets were surrounded by the bulk polymer matrix which had no chain alignment according to the results of Figs. 4 and 5. This resulted in poor alignment, as shown in the transmittance data of Fig. 2. Moreover, the degree of elastic distortion in the droplets depended on the gradient of curvature; a larger gradient of curvature (i.e., smaller droplet size) induces a more distorted molecular alignment in the droplets. Therefore, we could obtain a well-aligned PDFLC sample for droplet sizes larger than 1  $\mu\text{m}$ . However, this argument did not completely explain the decrease of alignment quality as the droplet size increased to 3  $\mu\text{m}$ .

Next we considered the droplet shape which is also closely related to the elastic distortion. Though 1 and 3  $\mu\text{m}$

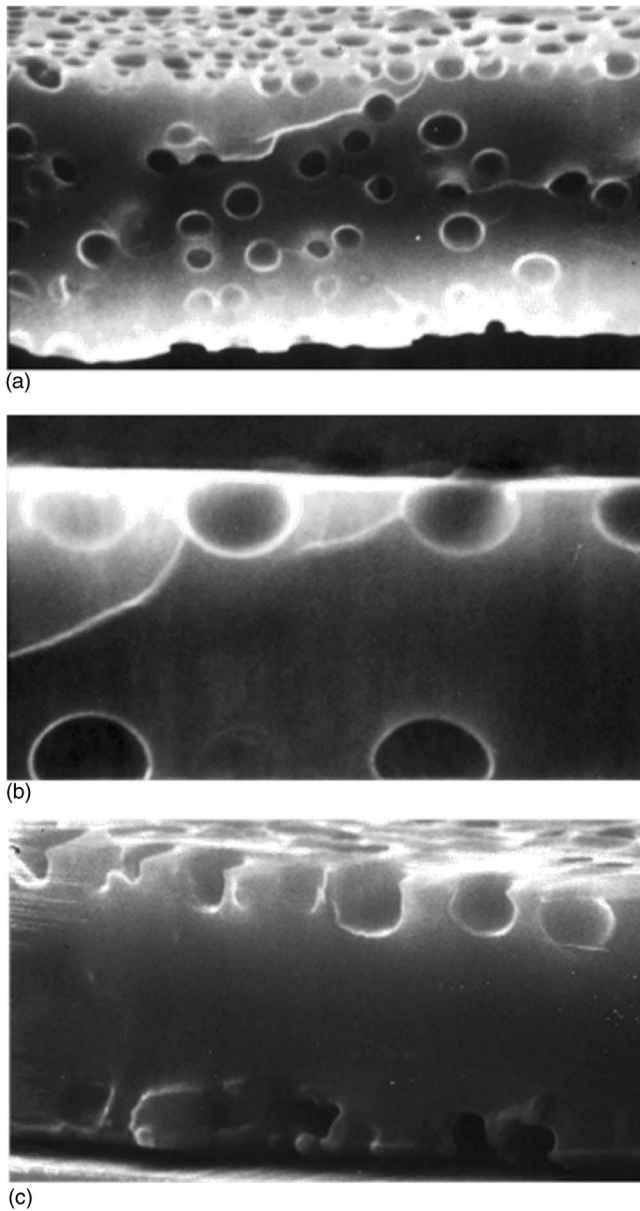
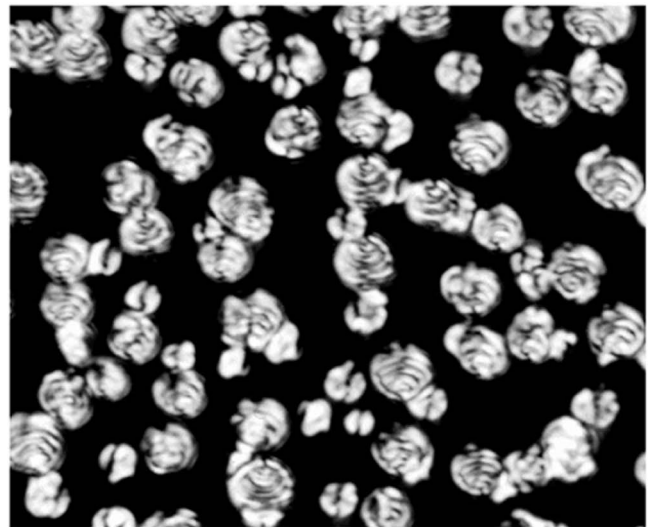


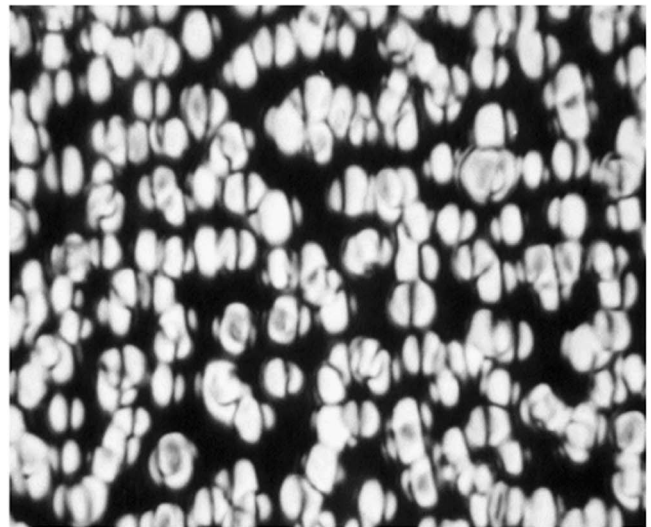
FIG. 6. The cross-sectional morphology as observed by SEM for droplet sizes of (a) 1, (b) 3, and (c) 7  $\mu\text{m}$  sample, respectively.

droplets had shapes that were almost spherical, the shape of the 7  $\mu\text{m}$  droplet was irregular as shown in Fig. 6(c). This irregularity was probably due to the fact that the PIPS process is unstable under the low uv intensity necessary to make a large droplet, 1  $\text{mW}/\text{cm}^2$  for a 7  $\mu\text{m}$  sample. In the spherical droplets the LC molecules experienced the same surface anchoring forces near the droplet wall. In the irregularly shaped droplets, however, the surface anchoring forces at various locations placed conflicting demands on the LC. The LC molecules can accommodate these forces in different ways through combinations of disclinations, splays, twists, and bends. Therefore, the irregular shapes as well as the large gradient of curvature contributed to the increased elastic distortion in the droplets. This could be one of the reasons for the existence of an optimum droplet size.

The alignment in the FLC droplets was also affected by the physical properties of the FLC such as the helical pitch,



(a)



(b)

FIG. 7. Photographs of the polarized microscopy image of (a) CS1017 and (b) CS1024 PDFLCs in the smectic- $C^*$  phase (200 $\times$  magnification).

phase sequence, and tilt angle. From the results of the PDCLC, the alignment of the LC molecules strongly depended on the helical pitch of the LC [17]. We made two PDFLC samples, one of which (CS1017) had a tight pitch (1  $\mu\text{m}$ ) with respect to the droplet size, and the other (CS1024) a relatively long helical pitch ( $>20 \mu\text{m}$ ) in the smectic- $C^*$  phase. We represented the texture of CS1017 and CS1024 samples in Fig. 7. For the texture observation, the droplet sizes were controlled to be 10–12  $\mu\text{m}$ . In the Sm-A phase, both samples showed the same defect structure, which meant that the smectic layers were well aligned for both samples. In Fig. 7(a) we represented the texture of CS1017 in which  $P/\rho \sim 0.1$  where  $P$  is the helical pitch. As shown in the figure, the defect lines were as complex as those of the PDCLC. This meant that the alignment of the FLC molecules in the droplets was greatly influenced by the helical structure in the regime of  $P/\rho < 1$ . But in the case of  $P/\rho > 1$ , the texture of CS1024 had the same line defects in almost all

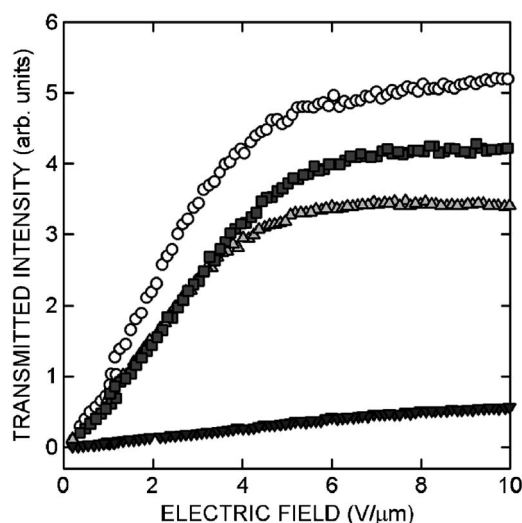


FIG. 8. The optical transmission for CS1024 as a function of the electric field.

droplets, which indicated better alignment than that of CS1017 as shown in Fig. 7(b).

Based on the above results, we concluded that the quality of alignment in the case of  $P/\rho > 1$  was determined by the droplet size and shape, and for the case of  $P/\rho < 1$ , the quality of alignment was determined by the helical structure. If we developed a method to make stable polymerization even under a low uv intensity and used the FLC compounds which had a long helical pitch in the Sm-C\* phase, we could make a larger optimum droplet size, and thereby improve the contrast ratio of the PDFLC.

Next to be considered was the EO response of the PDFLCs of various droplet sizes to an external electric field. The EO response was measured by monitoring the change in the transmitted light intensity through the sample cell between crossed polarizers. Measurements were made with a 50 Hz square wave of variable amplitude. Figure 8 shows the optical transmission curves for different droplet sizes. As we discussed above, the maximum transmittance was achieved with 3  $\mu\text{m}$  sample. All the curves showed a nearly linear EO effect at a relatively low electric field. By increasing electric field above 4 V/ $\mu\text{m}$ , the transmission became saturated. This resulted from a continuous unwinding of the helix and from the orientation of the molecules in the field direction, keeping the cone angle (or tilt angle) fixed. For the 1  $\mu\text{m}$  sample, the optical transmission denoted by the inverse triangular symbols was greatly suppressed. This means that the large elastic distortion by the large curvature of the droplet makes it hard to align the smectic layers and molecules. Figure 9 shows the field-driven rise times for various droplet sizes, except for the 1  $\mu\text{m}$  sample, which had relatively small transmission as a function of the electric field  $E$ . As we reported previously, the field-driven response time  $\tau_{on}$  is given by  $\tau_{on} = \eta / [PE + K(l^2 - 1)/a^2]$  where  $\eta$  is the associated viscosity,  $K$  is the effective elastic constant, and  $P$  is the spontaneous polarization. Here  $l = a/b$  denotes the aspect ratio of the droplet with  $a$  the semimajor axis and  $b$  the semiminor axis. Since  $\tau_{off} = \eta a^2 / K(l^2 - 1)$  is field independent, the response time  $\tau_{on}$  takes the form of

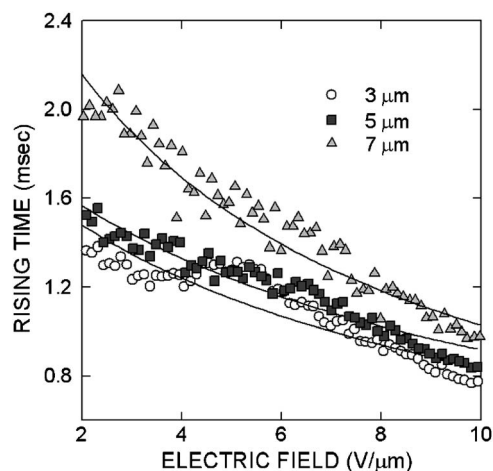


FIG. 9. The EO switching time for CS1024 as a function of the electric field.

$1/(PE/\eta + 1/\tau_{off})$ . The solid lines in Fig. 9 are the least-squares fits of the data. The fitted values for various droplet sizes are shown in Table I. By using the triangular wave method, the spontaneous polarization is measured as  $P \sim 1 \text{ nC/cm}^2$ , which is an order of magnitude smaller than those in the bulk. This is attributed to the confinement effect [13]. Accordingly, the associated viscosities for various droplet sizes were found to be in the range of 0.14–0.18 kg/m s, as shown in Table I, which are in good agreement with values reported in the literature [16]. Since molecular dynamics in restricted geometry is affected by bulk dynamics and the surface interaction between molecules and the droplet wall, the associated viscosity increased with decreasing droplet size. The relaxation times determined from the elastic properties decreased as the droplet size increased. In confined geometry, the equilibrium orientation of molecules is governed by the competition between surface interactions at the LC/polymer interface and the elastic properties of the LC. With a strong electric field to overcome the stable state, the molecules are aligned by the linear coupling of the electric field and dipole moment. Under the circumstances, a larger elastic distortion as well as a surface interaction makes a larger restoring force for the equilibrium state in the absence of an external electric field. Therefore, the relaxation times of the smaller droplets were faster than those of larger droplets.

#### IV. CONCLUDING REMARKS

We must note that our experimental results were different from those of shear aligned PDFLCs. In shear aligned

TABLE I. Fitting parameters used in Fig. 9.

Parameter	Size		
	3 $\mu\text{m}$	5 $\mu\text{m}$	7 $\mu\text{m}$
$P/\eta(10^{-5} \text{ m/V s})$	$5.81 \pm 0.30$	$6.41 \pm 0.26$	$6.91 \pm 0.20$
$\tau_{off} \text{ (ms)}$	$1.68 \pm 0.04$	$2.02 \pm 0.05$	$3.26 \pm 0.11$
$\eta \text{ (kg/ms)}$	$0.18 \pm 0.01$	$0.16 \pm 0.01$	$0.14 \pm 0.00$

PDFLCs, though the alignment also varied with droplet size, it did not change as much as in our rubbed samples [8]. The angular dependence of transmitted intensity modulation was varied continuously, and the maximum value was nearly independent of the droplet size in the same shear condition. In those samples, the alignment of the smectic layer was more strongly affected by shear strength. We suppose that these differences are primarily due to two factors. The first factor is the shape of the droplets. Because of the thermal treatment in our PDFLC samples, the droplet shapes were nearly spherical. In shear aligned PDFLC samples, however, the shape of the droplet was primarily ellipsoidal due to shear effects. The second factor is the boundary conditions. Even though the molecular alignments in the droplets were induced by a rubbed surface in our sample, those in the shear aligned sample were achieved by the anisotropic droplet shape and shear flow. As a result, the different droplet shapes and the different boundary conditions at the LC/polymer interface produced different PDFLC properties.

In summary, we have studied the layer alignment and the EO modulation in PDFLCs of different droplet sizes. There existed an optimum droplet size for maximum EO modulation and layer alignment, which was due to the elastic distortion of the FLC layer and surface interaction of the LC/polymer interface in the droplet. We found that the LC

molecules and layers were aligned by the aligned polymer near the surface which was promoted by a rubbed surface. The quality of alignment in the case of  $P/\rho > 1$  is determined by the droplet size and shape, though that in the case of  $P/\rho < 1$  is determined by the helical structure. We have presented the linear EO effect in the PDFLC composites of various droplet sizes. The associated ferroelectric switching was strongly dependent on droplet size. The effect of confinement of the FLC droplets on the EO response in the polymer matrix is primarily governed by microscopic molecular properties of the FLCs, such as the pitch in the Sm  $C^*$  state as well as the droplet shape and size. As the size of droplets decreased, the hindrance of the collective molecular rotation became profound, and thus the relaxation phenomenon in the restricted geometry appeared to be quite different from that in the bulk. Finally, for practical display applications, the method used to make stable polymerization even under low uv intensity and using long helical pitch would be useful to make a larger optimum droplet size, and it improves the contrast ratio of PDFLCs.

#### ACKNOWLEDGMENT

This work was supported by the Korea Research Foundation Grant No. KRF-2004-005-D00165.

- 
- [1] P. S. Drzaic, *J. Appl. Phys.* **60**, 2142 (1986).
  - [2] J. W. Doane, N. A. Vaz, B.-G. Wu, and S. Zumer, *Appl. Phys. Lett.* **48**, 269 (1986).
  - [3] J. H. Erdmann, S. Zumer, and J. W. Doane, *Phys. Rev. Lett.* **64** 1907 (1990).
  - [4] S. C. Jain and D. K. Rout, *J. Appl. Phys.* **70**, 6988 (1991).
  - [5] G. W. Smith, *Phys. Rev. Lett.* **70**, 198 (1993).
  - [6] S. C. Jain, R. S. Thakur, and S. T. Lakshmi Kumar, *J. Appl. Phys.* **73**, 3744 (1993).
  - [7] H.-S. Kitzerow, H. Molsen, and G. Heppke, *Appl. Phys. Lett.* **60**, 3093 (1992).
  - [8] H. Molsen and H.-S. Kitzerow, *J. Appl. Phys.* **75**, 710 (1994).
  - [9] K. Lee, S.-W. Suh, S.-D. Lee, and C. Y. Kim, *J. Korean Phys. Soc.* **27**, 86 (1994).
  - [10] K. Lee, S.-W. Suh, and S.-D. Lee, *Appl. Phys. Lett.* **64**, 718 (1994).
  - [11] A. M. Lackner, J. D. Margerum, and K.-C. Lim, *Proc. SPIE* **1080**, 53 (1989).
  - [12] G. P. Montgomery, Jr., J. L. West, and W. Tamura-Lis, *J. Appl. Phys.* **69**, 1605 (1991).
  - [13] J. H. Kim, K. Lee, S.-W. Shu, Y. Kim, and S.-D. Lee, *J. Korean Phys. Soc.* **27**, S115 (1994).
  - [14] J. H. Kim (unpublished results).
  - [15] G. S. Iannacchione and D. Finotello, *Phys. Rev. Lett.* **69**, 2094 (1992).
  - [16] Chisso Petrochemical Corp., Chiba, Japan.
  - [17] Z.-J. Lu and D.-K. Yang, *Appl. Phys. Lett.* **65**, 505 (1994).
  - [18] D. Nwabunma, H.-W. Chiu, and T. Kyu, *J. Chem. Phys.* **113**, 6429 (2000).